# Influence of fuel ratio on synthesis and characterization of LaCoO3 perovskite nanoparticles by sol-gel auto-combustion method

Hamed Sadabadi[1], Saeed Allahkaram[1], Amir Kordijazi[2], Omid Akbarzadeh[3], and Pradeep Rohatgi[2]

[1]University of Tehran College of Engineering
[2]University of Wisconsin Milwaukee
[3]University of Malaya

May 5, 2020

## Abstract

Recently, nanostructure perovskite oxides such as LaMO3 (M=Co, Ni, Fe, . . . ) received attention in academic researches due to its catalytic properties. In this research, the LaCoO3 perovskite nanoparticles have been synthesized by single-step route via the sol-gel auto-combustion method. The precursors used in this method were lanthanum nitrate and cobalt nitrate, as metals sources dissolved in distilled water and also using PVP as a surfactant, Urea and glycine as an oxidizer. The sol formed at stirring stage at 60 °C continued by gelation through the water evaporation at 90 °C and then auto-combustion occurred. Product of combustion step was washed and centrifuged three times and later calcined at 600 °C for 2 h. As synthesized nanoparticles are characterized by scanning electron microscopy (SEM), X-ray powder diffraction (XRD), and particle size analyzer (PSA). The characterization results proved the synthesis of nanoparticles below 100 nm with perovskite structure in narrow size distribution by using this method. The purity and size of nanoparticles vary depending on the fuel and fuel to oxidizer ratio.

*Keywords: Sol-gel auto-combustion, Nanoparticles, Perovskite, characterization, LaCoO$_3$*

## Introduction:

Metal oxide Nanoparticles have certain industrial and technological properties that include optical, magnetic, electrical, catalytic, mechanical strength, thermal stability and chemical properties. The production of metal oxide nanoparticles is carried out using a number of chemical methods, which include sol-gel, reduction-oxidation, hydrothermal hydroxide oxidation, and metal salts decomposition methods. Time efficiency, production cost, ability to operate continuously, and production rate are the parameters that have been considered in order to choose the best synthesis method for a specific application. Solution combustion synthesis (SCS) or sol-gel auto-combustion method appears to be a promising method due to low production cost, because it requires low-cost precursor materials and equipment. It's feasible to fabricate a wide range of nanoparticles and metal oxides, and more efficiently compared to some other methods [1]–[5].

The perovskite oxides are mixed metal oxides with the general formula of ABO$_3$, where A is larger cation usually an alkaline-earth or rare-earth metal cation and B is the smaller cation, usually, a transition-metal cation (e.g., Mn, Co, Fe, Ni,) surrounded by six oxygen atoms in an octahedral coordination [6]. However, perovskite oxides, LaMO$_3$, in which M is a transition-metal containing Co, Fe, Ni, have been used in a variety of applications, including gas sensors (CO, propane and ethanol sensing) as nanostructures' film, hollow spheres and mesoporous nanowires, nanoparticles, porous and fibrous structures [7]–[11], photocatalytic reduction of CO$_2$ with visible light, electronic devices, electrochemical systems, solid oxide fuel cell, solar cells, and catalysts [11]–[17]. Different methods have been uses to synthesize and develop perovskite phase of

1

$LaCoO_3$ as nanoparticles and nanowires, over the years; these include thermal decomposition, hydrothermal, microwave-assisted coprecipitation, co-precipitation, sol-gel, and combustion methods [10], [17]–[22].

The purpose of this research is to synthesize nanoparticles of $LaCoO_3$ perovskite in a single step by combining the sol-gel and auto-combustion steps. Investigation of the influence of fuel ratio and different fuel on nanoparticle characteristics has been done. These particles can be used as a catalyst in the decomposition of nitrogen oxide gases (NOx).

**Experimental:**

The following materials were used as precursors for synthesis of perovskite particles. Lanthanum Nitrate $(La(NO_3)_3\text{-}6H_2O)$ and Cobalt Nitrate $(Co(NO_3)_2\text{-}6H_2O)$ as a supplier of metal elements, glycine $(C_2H_5NO_2)$ and urea $(CH_4N_2O)$ as fuel, and PVP as a surfactant were used in these experiments. All of the precursor materials were purchased from Merck-Germany and used in the experiments without further purification.

Firstly, 0.1M solutions of lanthanum nitrate and cobalt nitrate was prepared in 100 ml of distilled water in a 250 ml beaker and stirred on a magnetic stirrer for 15 minutes until the material was completely dissolved and a uniform pink solution was obtained. In the second step, four different samples were prepared, as shown in Table 1. The stoichiometric amount of glycine and urea were added slowly to the solution. The glycine/metal and urea/ metal ratio were kept 1 and 2 in this experiment (F/O=1 & 2). The solution temperature was increased to 60 °C and PVP by 5% by weight of the available metals was added. PVP played the role of surfactant in the experiment, to help obtain a uniform shape and narrow size distribution. Solutions were mixed using vigorous stirring on a magnetic stirrer for half an hour. The next step was combustion. At this stage, the solution temperature was increased up to 90 °C in order to evaporate water slowly, followed by gelation and combustion. The solution was stirred using a magnetic stirrer, until combustion occurred.

The powder was washed with distilled water and centrifuged at 2000 RPM for 15 minutes for three times, and collected nanoparticles were calcined at 600 °C for 2 hours in a furnace.

Table 1: experimental conditions.

| Sample No. | Fuel | F/O ratio | Metal solution Molarity | PVP |
|---|---|---|---|---|
| LCG 1 | Glycine | 1 | 0.1M | 5%wt |
| LCG 2 | Glycine | 2 | 0.1M | 5%wt |
| LCU 1 | Urea | 1 | 0.1M | 5%wt |
| LCU 2 | Urea | 2 | 0.1M | 5%wt |

During the experiment, all parameters that influence the properties of nanoparticles were kept constant, just fuel and fuel to oxidizer ratio used as variable parameters, and influence of these two parameters was studied.

**Results**

X-ray powder diffraction (XRD) patterns were recorded by a D8 Advance (Bruker) with Cu Kα (wavelength 1.54 Å) after nanoparticles were calcined at 600 °C for 2 hours. SEM (FEI Company, USA-Quanta 200) was used to investigate the morphology, size, and uniformity of the products. A particle size analyzer was used to illustrates the size distribution. During the PSA test, the ethanol was used as a dispersant, temperature was set at 25 °C, and the test duration was 50 s.

The powder XRD data are shown in Fig.1(a-b) and Fig.2(a-b), indicates the crystalline structure of the as-synthesized perovskite-type oxide nanoparticles obtained using the sol-gel auto-combustion method. The ratio of fuel to oxidizer (F/O), and using different fuel in this method, causes the changes crystalline properties and purity of the final product. However, XRD patterns of all samples exhibited diffraction peaks of $LaCoO_3$ (JCPDS No.-01-084-0848), irrespective of the F/O ratio and fuel. But the existence of impurity was observed and discussed as follows. Fig.1(a-b) shows the XRD patterns of sample LCG1 and LCG2 respectively. As

2

illustrated in Fig.1-a, by using glycine in the ratio of F/O=1, the mixture of the cobalt oxide (CoO, $Co_3O_4$), lanthanum oxide ($La_2O_3$), $La(OH)_3$ and perovskite phase obtained, but Fig1-b shows the purity of perovskite phase. It was shown strong peaks at 32.9° (110) and 33.3° (104), and the peaks observed around 32°, 60° and 70° are bifurcated which is the characteristic peak for the rhombohedral structure and also indicated no trace of CoO, $Co_3O_4$, $La(OH)_3$ or $La_2O_3$, which corresponded to the high degree of La and Co oxide incorporation into the perovskite structure achieved by glycine as fuel and F/O=2. Furthermore, Fig.2 (a-b) shows that using urea as fuel can cause changes in purity and crystalline properties also. The production of $LaCoO_3$ nanoparticles, with $Co_3O_4$ and $La_2O_3$ as impurities by using both F/O=1 and 2 was achieved. However, it can be concluded that higher ratio of glycine causes complete oxidation while urea in low ratio and high ratio cause partial oxidation and lower degree of La and Co oxide incorporation into the perovskite structure.
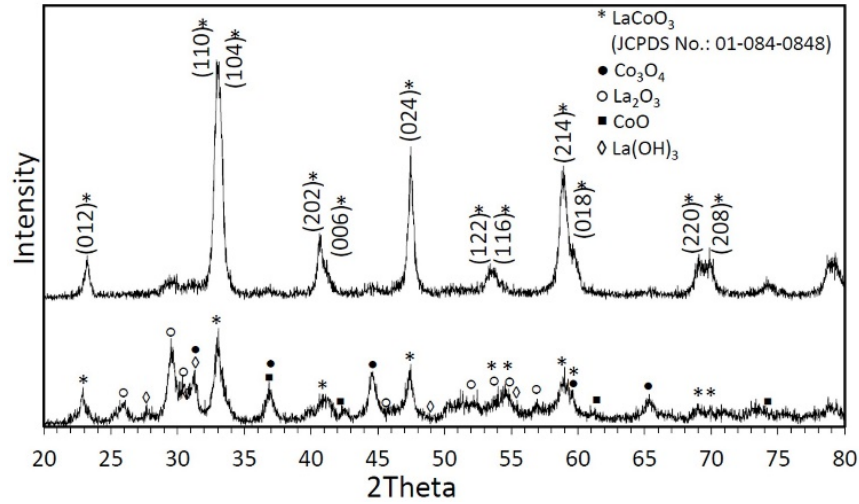


Fig.1: XRD patterns of $LaCoO_3$ nanoparticles, using glycine as fuel and calcined at 600°C in air a) sample LCG1 F/O=1, b) sample LCG2 F/O=2.
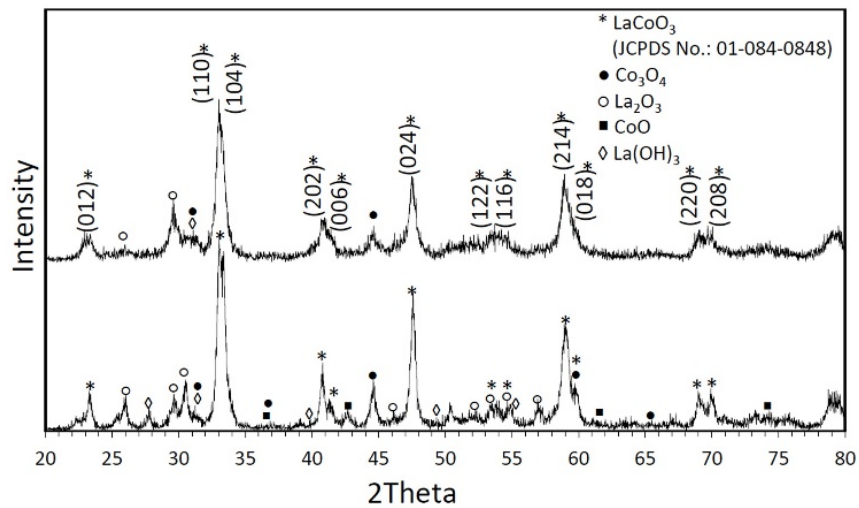
3

Fig.2: XRD patterns of LaCoO₃ nanoparticles, using urea as fuel and calcined at 600°C in air a) sample LCU1 F/O=1, b) sample LCU2 F/O=2.

Finally, crystallite size and the average crystallite size was estimated according to the Debye and Scherrer formula from the (110), (024) and (214) reflection of the LaCoO₃ phase at 2q[?] 32.9deg, 47.5deg and 58.9deg respectively, and is represented in Table 2.

$D = \frac{0.94\lambda}{\beta\cos\theta}$ (1)

Where:

D is the crystallite size

λ is the X-ray wavelength (1.5418 Å)

β is the full width of the half maximum (FWHM) of the diffraction peak

ϑ is the Bragg diffraction angle

It was evident from the calculation that LaCoO₃synthesized using glycine exhibited the lowest crystallite size (~14.9 and 28.1 nm) compared to when urea was used (~41.6 and 25.7 nm). The larger crystallite size of the LaCoO₃ phase observed in the LCU1 sample was indicative of the greater growth of its crystal domains. This result reveals that glycine and urea act in opposite manner, while increasing fuel ratio in glycine increase the crystallite size and purity, increasing urea decreases crystallite size and improves purity.

Table 2. Crystallite size, average crystallite size and Z-average size of four samples synthesized with different fuel and fuel to oxidizer ratio (F/O).

|  | LCG1 | LCG2 | LCU1 | LCU2 |
|---|---|---|---|---|
| Crystallite size $D_{110}$ (nm) | 15.9 | 18 | 36.7 | 31.4 |
| Crystallite size $D_{024}$ (nm) | 18.9 | 37.8 | 57.7 | 25.6 |
| Crystallite size $D_{214}$ (nm) | 9.9 | 28.4 | 30.3 | 20.2 |
| Crystallite size $D_{Ave.}$ (nm) | 14.9 | 28.1 | 41.6 | 25.7 |
| PSA-average (d.nm) | 72.2 | 70.2 | 72.0 | 72.8 |
| Z-average (d.nm) | 104.1 | 97.9 | 101.9 | 106.5 |

Also, Results from particle size analyses shows the narrow size distribution as illustrated by Fig.3-4 and the SEM micrograph proves that.
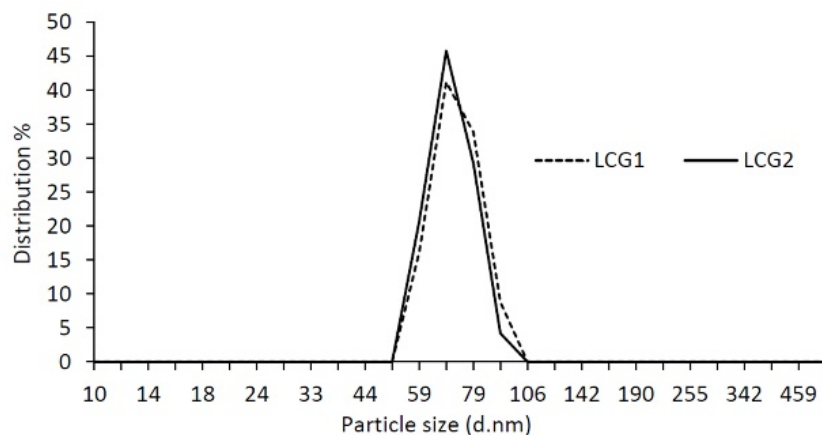
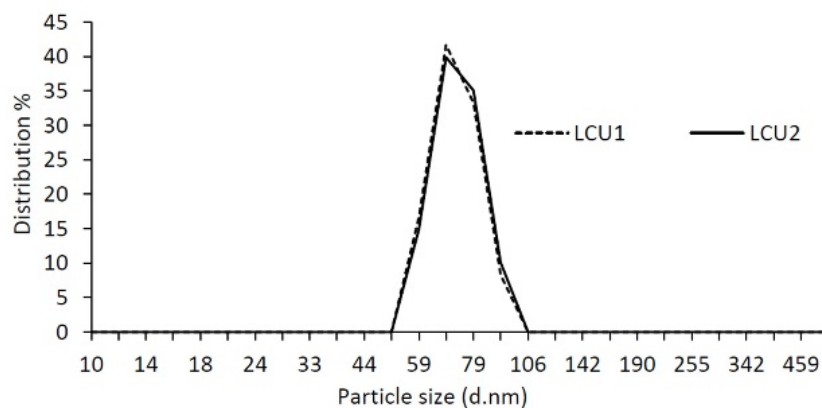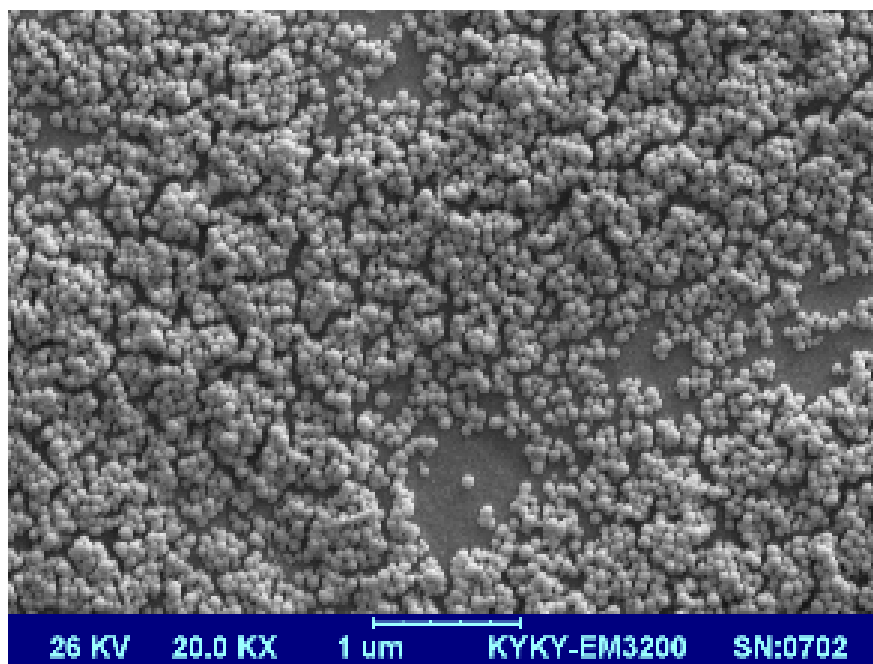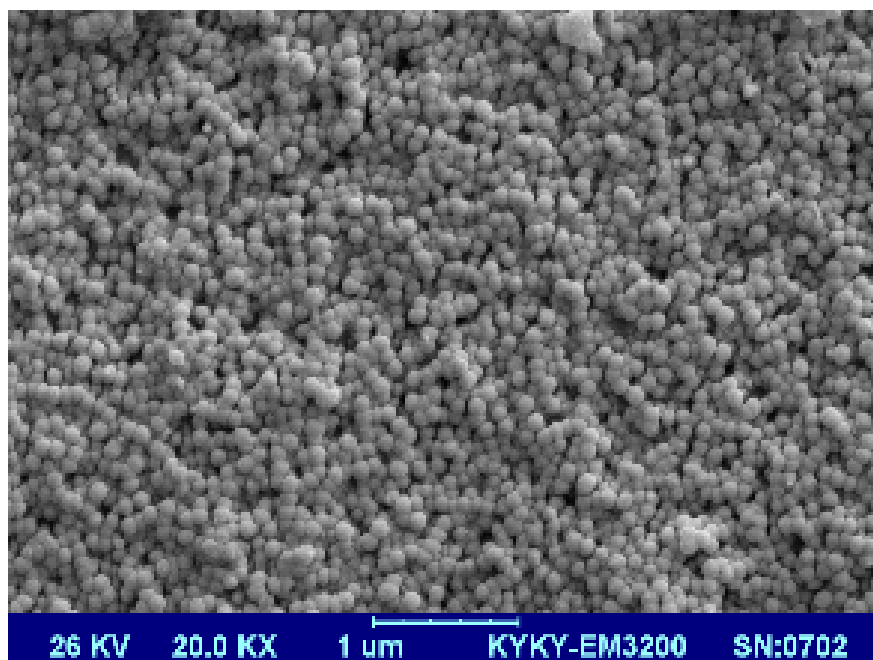Fig.3: PSA graph of sample LCG1(—) and LCG2 ( ).



Fig.4: PSA graph of a) sample LCU1(—) and sample LCU2( ).

Morphologies of $LaCoO_3$ synthesized with the sol-gel Auto-combustion method by glycine and urea as fuel are presented in Fig.5 (a-b) and Fig.6 (a-b), respectively. The SEM images show nonporous nature of the synthesized perovskite particles with spherical shape in all samples. The porous nature can be due to the nitrate precursors because burning of the nitrates at higher temperature may lead to the porous structures.

A comparison of these micrographs reveals that the glycine in ratio of 2 resulted in a lower particle size and homogeneity, while the powder prepared by the urea showed a relatively larger particle size, some agglomeration and inhomogeneity in shape and size is observed. The average particle size of LaCoO$_3$ synthesized by glycine is below 70 nm with a spherical shape, whereas the powder made of urea process has a broader particle size distribution and inhomogeneity in shape. However, SEM results are contradictory to the results of crystallite size estimation (see Table 2). Particle size is different from crystallite size suggesting that the particles have multi-crystalline structure. A particle may be made up of several different crystallites.
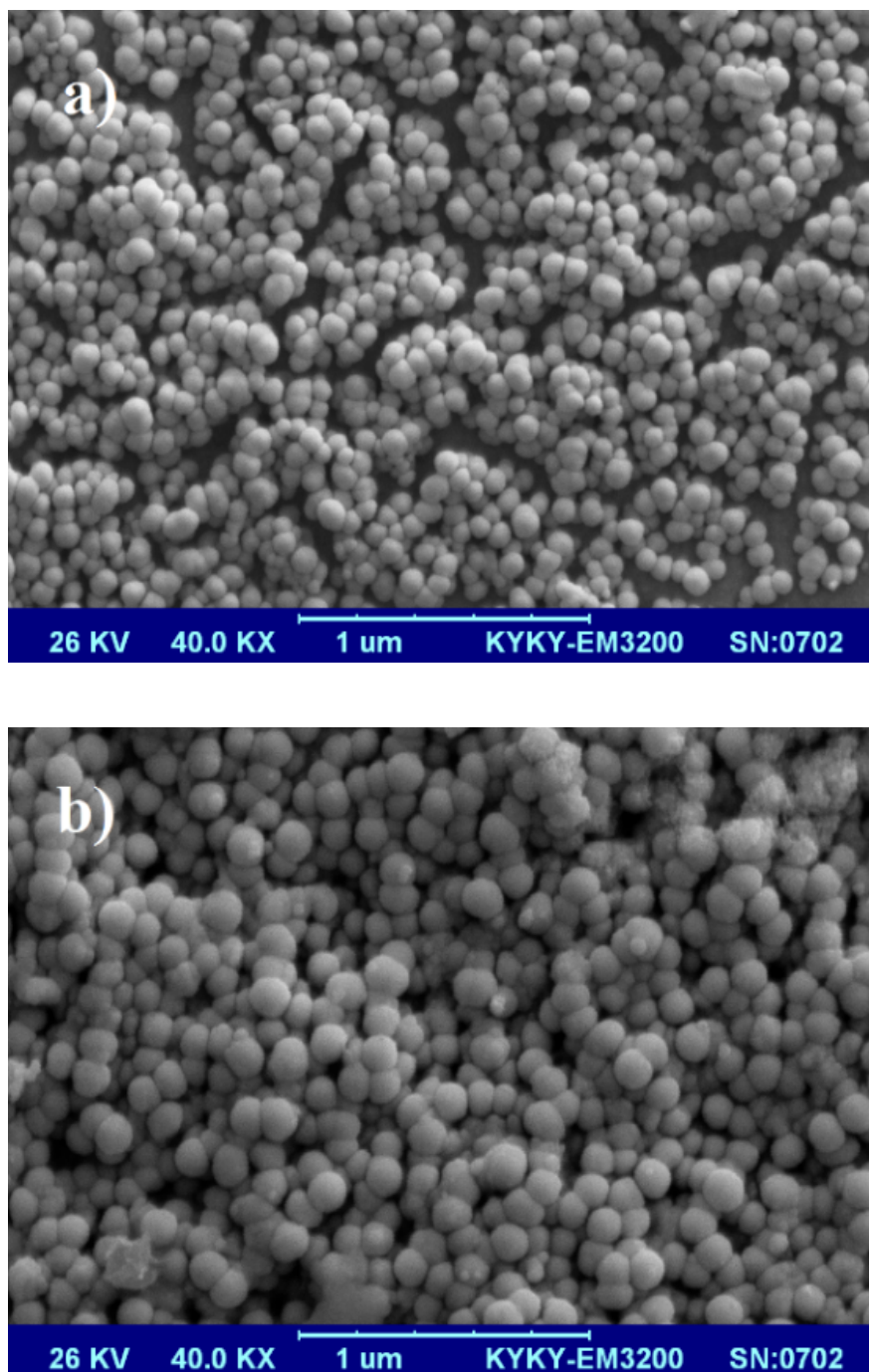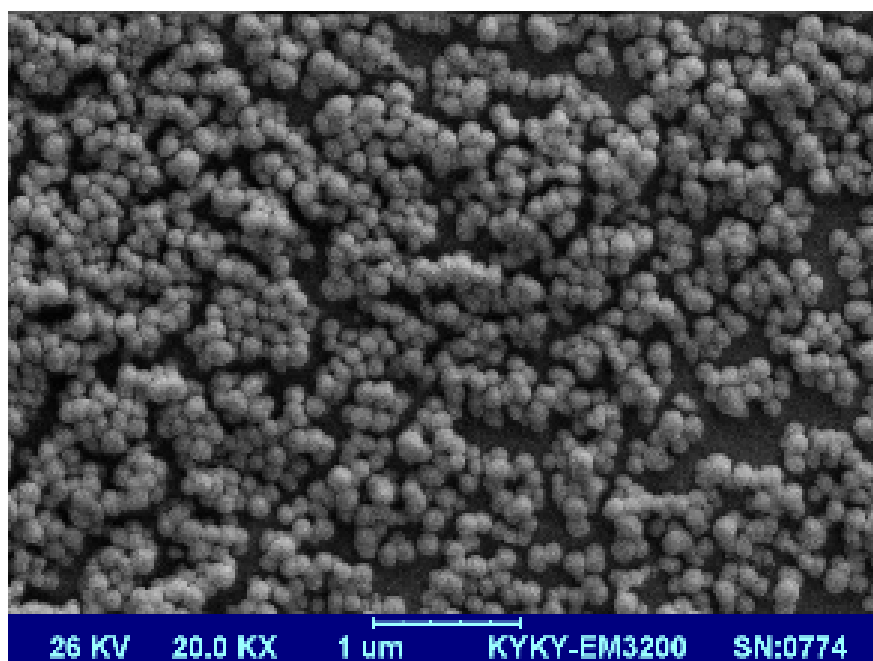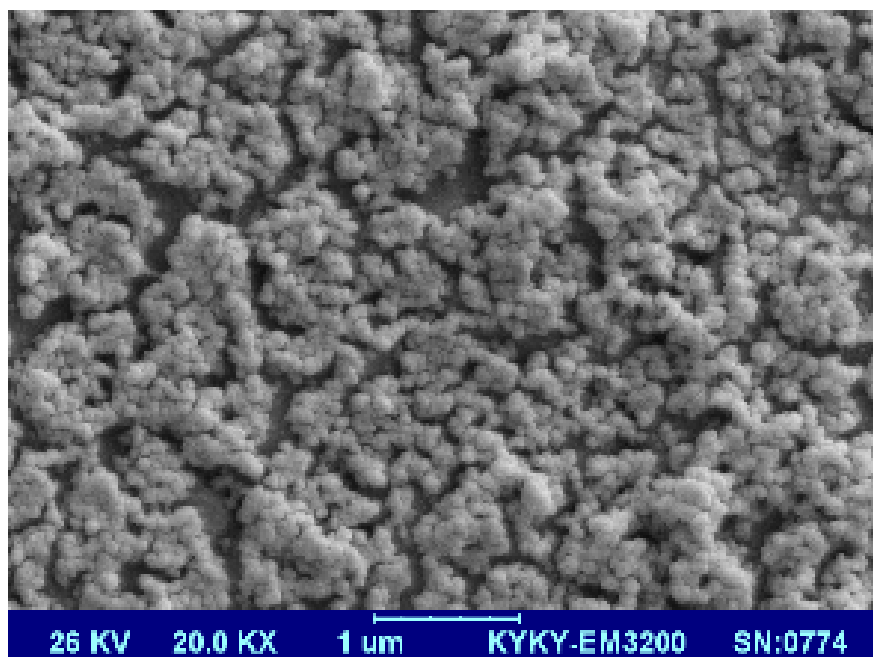
Fig.5: SEM micrograph of LaCoO$_3$ nanoparticles, using glycine as fuel and calcined at 600°C in air a) sample LCG1 F/O=1, b) sample LCG2 F/O=2.
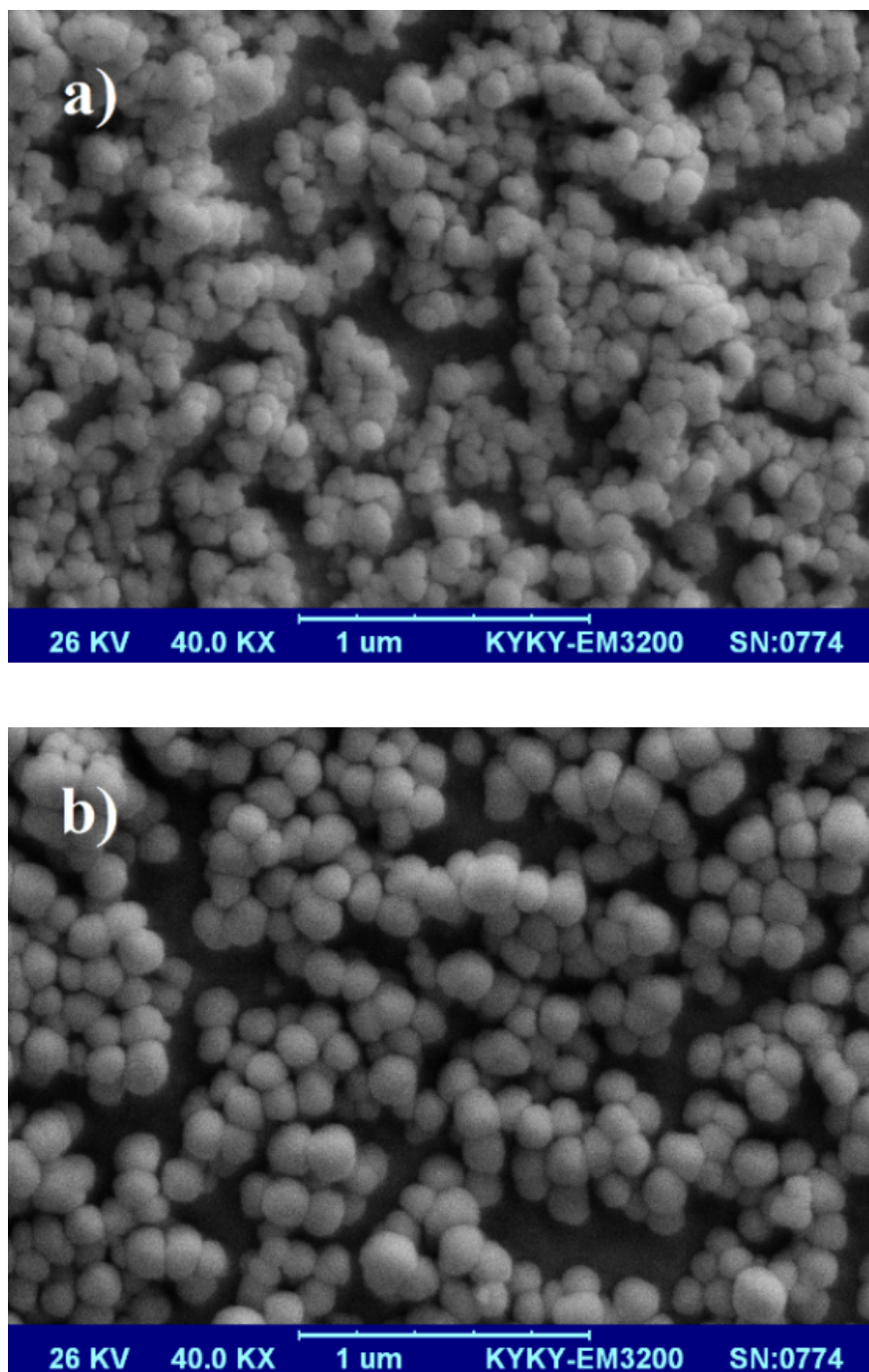
Fig.6: SEM micrograph of LaCoO$_3$ nanoparticles, using urea as fuel and calcined at 600°C in air a) sample LCU1 F/O=1, b) sample LCU2 F/O=2.

Also, Results from particle size analyses shows the narrow size distribution as illustrated by Fig.5 and 6 and the SEM micrograph proves that.

**Conclusion:**

LaCoO₃ perovskite nanoparticles can be produced by sol-gel auto-combustion, using a single step method. This method is low-cost, time-efficient and does not require advanced equipment for the production process. Investigation of the lattice structure, morphology, particle size by XRD, SEM and PSA analysis methods show that particles are uniform in shape and size and these characteristics play important roles in the application of nanoparticles as the catalyst and cause uniformity in the properties of the catalyst. The production of uniform size nanoparticles using this method is the result of the use of surfactants in the synthesis process. The results confirm the successful synthesis of LaCoO₃ nanoparticles which are in a spherical shape and below 100 nm in size.

**Conflict of Interest:**

Authors have no conflict of interest relevant to this article.

**References:**

[1] S. T. Aruna and A. S. Mukasyan, "Combustion synthesis and nanomaterials," *Curr. Opin. Solid State Mater. Sci.* , vol. 12, no. 3–4, pp. 44–50, 2008.

[2] T. Mimani and K. C. Patil, "SOLUTION COMBUSTION SYNTHESIS OF NANOSCALE OXIDES AND THEIR COMPOSITES," vol. 4, pp. 134–137, 2001.

[3] A. Varma, A. S. Mukasyan, A. S. Rogachev, and K. V Manukyan, "Solution Combustion Synthesis of Nanoscale Materials," 2016.

[4] H. Sadabadi, A. Aftabtalab, S. Zafarian, S. Chakra, K. V. Rao, and S. Shaker, "Influence of Fuel and Condition in Combustion Synthesis on Properties of Copper (II) Oxide Nanoparticle," in *Ultrafine Grained and Nano-Structured Materials IV* , 2014, vol. 829, pp. 152–156.

[5] H. Sadabadi, A. Aftabtalab, S. Zafarian, S. Shaker, M. Ahmadipour, and K. Venkateswara, "High purity Alpha Alumina nanoparticle : Synthesis and characterization," *Int. J. Sci. Eng. Res.* , vol. 4, no. 4, pp. 1593–1596, 2013.

[6] J. L. G. Fierro and V. I. Acknowledgment, "Chemical Structures and Performance of Perovskite Oxides," 2001.

[7] C. R. Michel, A. H. Martinez-Preciado, E. R. Lopez-Mena, A. Elias-Zuniga, N. Cayetano-Castro, and O. Ceballos-Sanchez, "Improvement of the gas sensing response of nanostructured LaCoO3 by the addition of Ag nanoparticles," *Sensors Actuators, B Chem.* , vol. 246, pp. 181–189, 2017.

[8] J. C. Ding, H. Y. Li, Z. X. Cai, X. X. Wang, and X. Guo, "Near room temperature CO sensing by mesoporous LaCoO3 nanowires functionalized with Pd nanodots," *Sensors Actuators, B Chem.* , vol. 222, pp. 517–524, 2016.

[9] L. Gildo-Ortiz *et al.* , "Key processing of porous and fibrous LaCoO3 nanostructures for successful CO and propane sensing," *Ceram. Int.* , vol. 44, no. 13, pp. 15402–15410, 2018.

[10] W. Haron, A. Wisitsoraat, and S. Wongnawa, "Nanostructured perovskite oxides – LaMO3 (M=Al, Co, Fe) prepared by co-precipitation method and their ethanol-sensing characteristics," *Ceram. Int.* , vol. 43, no. 6, pp. 5032–5040, 2017.

[11] S. Fu *et al.* , "Low temperature synthesis and photocatalytic property of perovskitetype LaCoO3 hollow spheres," *J. Alloys Compd.* , vol. 576, pp. 5–12, 2013.

[12] X. Huang, G. Zhao, G. Wang, and J. T. S. Irvine, "Synthesis and applications of nanoporous perovskite metal oxides," *Chem. Sci.* , vol. 9, no. 15, pp. 3623–3637, 2018.

[13] J. Qin, L. Lin, and X. Wang, "A perovskite oxide LaCoO3 cocatalyst for efficient photocatalytic reduction of CO2 with visible light," *Chem. Commun.* , vol. 54, no. 18, pp. 2272–2275, 2018.

[14] S. U. Rehman *et al.* , "High-performance nanofibrous LaCoO3 perovskite cathode for solid oxide fuel cells fabricated: Via chemically assisted electrodeposition," *J. Mater. Chem. A* , vol. 6, no. 16, pp. 6987–6996, 2018.

[15] B. Seyfi, M. Baghalha, and H. Kazemian, "Modified LaCoO3 nano-perovskite catalysts for the environmental application of automotive CO oxidation," *Chem. Eng. J.* , vol. 148, no. 2–3, pp. 306–311, 2009.

[16] J. Yang and Y. Guo, "Nanostructured perovskite oxides as promising substitutes of noble metals catalysts for catalytic combustion of methane," *Chinese Chem. Lett.* , vol. 29, no. 2, pp. 252–260, 2018.

[17] C. Alvarez-Galvan *et al.* , "Microwave-assisted coprecipitation synthesis of LaCoO3 nanoparticles and their catalytic activity for syngas production by partial oxidation of methane," *Front. Energy Res.* , vol. 6, no. APR, pp. 1–11, 2018.

[18] W. Kaituo, W. Xuehang, W. Wenwei, L. Yongni, and L. Sen, "Synthesis of perovskite LaCoO3 by thermal decomposition of oxalates: Phase evolution and kinetics of the thermal transformation of the precursor," *Ceram. Int.* , vol. 40, no. 4, pp. 5997–6004, 2014.

[19] L. Tepech-Carrillo *et al.* , "Preparation of Nanosized LaCoO3 through Calcination of a Hydrothermally Synthesized Precursor," *J. Nanomater.* , vol. 2016, 2016.

[20] A. D. Jadhav, A. B. Gaikwad, V. Samuel, and V. Ravi, "A low temperature route to prepare LaFeO3 and LaCoO3," *Mater. Lett.* , vol. 61, no. 10, pp. 2030–2032, 2007.

[21] Y. Wang, X. Yang, L. Lu, and X. Wang, "Experimental study on preparation of LaMO3 (M = Fe, Co, Ni) nanocrystals and their catalytic activity," *Thermochim. Acta* , vol. 443, no. 2, pp. 225–230, 2006.

[22] A. Ashok *et al.* , "Combustion synthesis of bifunctional LaMO3 (M = Cr, Mn, Fe, Co, Ni) perovskites for oxygen reduction and oxygen evolution reaction in alkaline media," *J. Electroanal. Chem.* , vol. 809, no. December 2017, pp. 22–30, 2018.